A DB RILEY TECHNICAL PUBLICATION

EVALUATION OF HOT REHEAT STEAM PIPING, INCLUDING A TEST SPOOL PIECE, AT THE BIG CAJUN II STATION

by

Robert Hendrix, Senior Engineer
Cajun Electric Power Co-operative, Inc.

and

Joyce M. Khoury, Senior Metallurgist

James P. King, Design Manager

Brian Ryder, Senior Engineer
DB Riley, Inc.

Presented at the
POWER-GEN'96 International
December 4-6, 1996
Orlando, Florida

RST-144

DEUTSCHE BABCOCK

DB RILEY, INC.

Post Office Box 15040
Worcester, MA 01615-0040
http://www.dbriley.com

EVALUATION OF HOT REHEAT STEAM PIPING, INCLUDING A TEST SPOOL PIECE, AT THE BIG CAJUN II STATION

by

Robert Hendrix, Senior Engineer
Cajun Electric Power Co-operative, Inc.
and
Joyce M. Khoury, Senior Metallurgist
James P. King, Design Manager
Brian Ryder, Senior Engineer
DB Riley, Inc.

ABSTRACT

This paper provides an overview of a portion of Cajun Electric Power Co-operative's ongoing program for the evaluation of the major steam piping line supports and components in the three units at their Big Cajun II Station in New Roads, Louisiana.

During the course of this continuing evaluation program, indications were detected in the girth and longitudinal seam welds on a portion of hot reheat piping of Unit No. 1. In order to more closely define these indications and to provide an assessment of the current condition of the piping and weldment materials, a three-foot-long piece of the hot reheat pipe was removed for a comprehensive analytical and testing program. This program, the primary focus of the paper, includes the following items:

- *Review Fabrication, Construction and Operating History*
- *Visual Inspection of the Spool Piece*
- *Ultrasonic Testing of Longitudinal and Circumferential Welds*
- *Wet Fluorescent Magnetic Particle Testing*
- *Radiographic Inspection of the Welds*
- *Metallurgical Investigation*
- *Mechanical Testing*
- *Remaining Life Evaluations*

The paper will present the current results of this extensive analytical and testing program.

INTRODUCTION

The object of this paper is to discuss the current findings of an ongoing program for the evaluation of the seam-welded hot reheat piping system at Cajun Electric Power Co-operative's Big Cajun II Station, Unit No. 1 in New Roads, Louisiana. During onsite inspection, indications were found by ultrasonic testing, and creep damage was observed by metallographic replication, in the long seam and girth welds in portions of the hot reheat piping, which resulted in the removal of plug samples for metallurgical evaluation. In lieu of performing a weld repair of the piping, and in order to study the indications more closely, a three-foot-long piece of the hot reheat piping was removed for a comprehensive analytical testing program. The program is the primary focus of this paper.

Background

The reheat piping from Big Cajun II, Unit 1 is fabricated from ASTM A155 - Class 2-1/4 alloy steel plate (governed by SA387 Grade D, 2-1/4 Cr - 1 Mo). It has a nominal inside diameter of 23 inches and a minimum wall thickness of 1.124 inches. The piping has a design temperature of 1015°F. Currently, Unit No. 1 undergoes operational load swings on a daily basis. Daily hot reheat pressures vary with megawatt load, typically ranging from 350 to 600 psig. Daily variations in hot reheat temperature may be from 940°F to 1015°F. At the time of removal of the spool piece in October of 1995, the piping had been in service for about 106,000 hours. The spool piece contains two portions of longitudinal welds, which are off-set and joined by a circumferential girth weld (Figures 1a and 1b).

The objective of this study is to assess the current condition of the component materials of the hot reheat piping in order to estimate the remaining useful life. The study can be broken down into three major tasks. Task One is the visual inspection and non-destructive testing of the spool piece in the laboratory. This task includes the wet fluorescent magnetic particle testing (WFMT) of the welds from the internal surface of the pipe. Gamma radiography was performed on all the welds. The welds were inspected using straight and angle beam ultrasonic techniques, per Electric Power Research Institute (EPRI) guidelines (See Ref. 1).

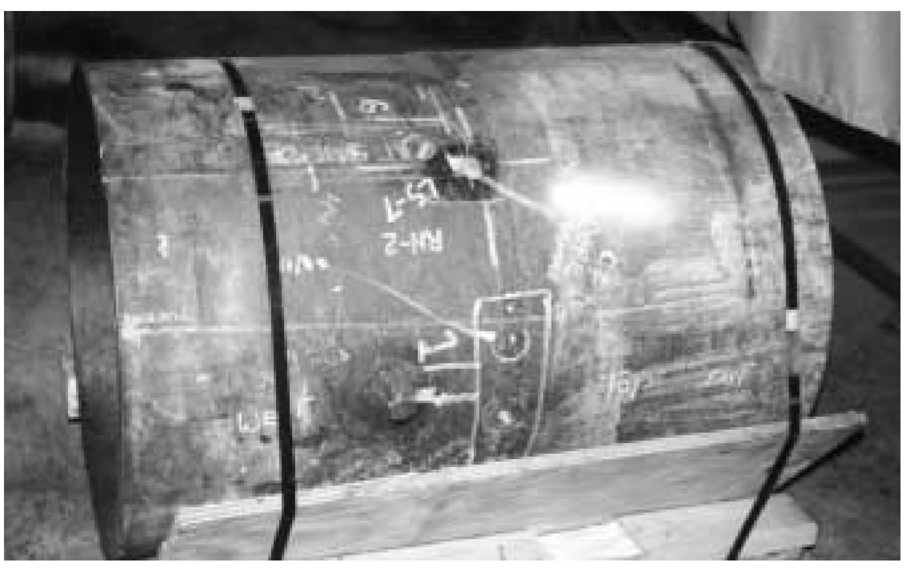

Figure 1a The Spool Piece As-received From the Hot Reheat Line at Big Cajun II Unit No. 1, Showing the Downstream Portion of the Seam Weld and the Locations of the Plug Samples in the Longitudinal and Circumferential Welds.

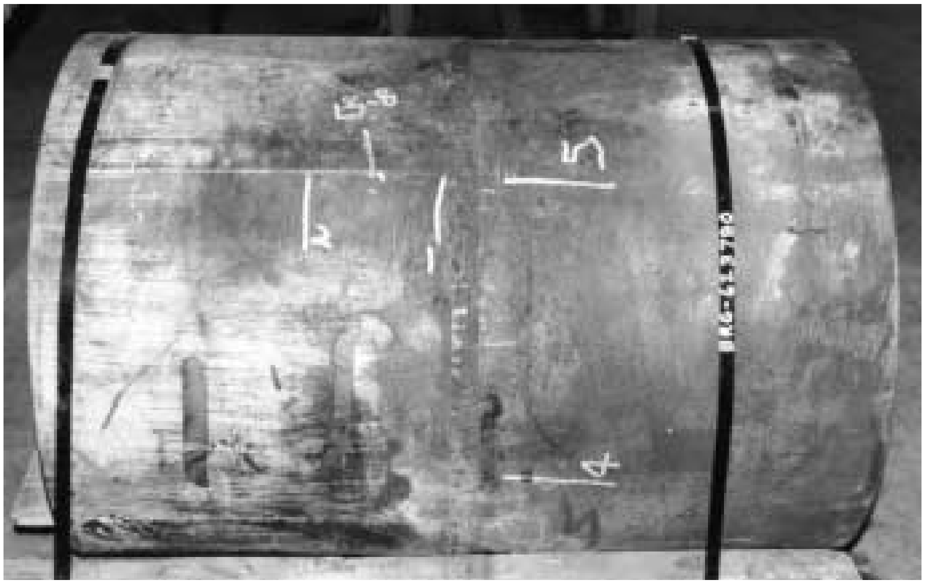

Figure 1b Photograph of the Spool Piece As-received From the Hot Reheat Line at Big Cajun II Unit No. 1, Showing the Upstream Leg of the Long Seam.

Task Two is the physical and chemical characterization of the base and weld metal of the spool piece components. Based on the NDE results, full cross-section weld specimens were selected for optical metallography and hardness testing. The elemental composition of samples of the base metal and long seam weld metal were determined to confirm alloy composition and to assess flux acidity. Scanning electron microscope (SEM) examination of the long seam metallographic sample has been done to determine the presence of any creep damage not resolved by light microscopy and for evidence of inclusion/particle segregation along the fusion line. The metallographically prepared stress-rupture specimens were also examined in the SEM. In addition, energy dispersive X-ray (EDS) analysis was performed to characterize non-metallic inclusions in the weld metal and heat-affected zone.

Task Three is comprised of mechanical testing to determine the stress-rupture and creep-crack-growth properties of the material. Cross-weld specimens were used for all phases of testing which included stress-rupture, elevated temperature toughness (J_{IC}) and creep-crack-growth (C*) testing. Metallographic specimens were prepared from the stress-rupture specimens to examine the fracture characteristics.

TASK ONE: VISUAL INSPECTION AND NON-DESTRUCTIVE TESTING

Visual Inspection

The spool piece, having nominal measured dimensions of 25-1/4" O.D. by 1-1/8" wall and 22-7/8" I.D., had been cut from the hot reheat line at a location downstream from a “Y” connection, which is inside the turbine building (Figure 1). The spool piece had been cut eighteen inches on each side of a circumferential (girth) weld and contained two offset portions of longitudinal seam weld (upstream [Figure lb] and downstream [Figure la] from the girth weld). The steam flow in the pipe is from east to west at this point in the line. A layout of the as-received spool piece is shown in Figure 2. The locations of the plug samples, which had been removed prior to removing the spool piece from the line, are indicated by the 1" radiographic holes in the girth weld and in the downstream seam.

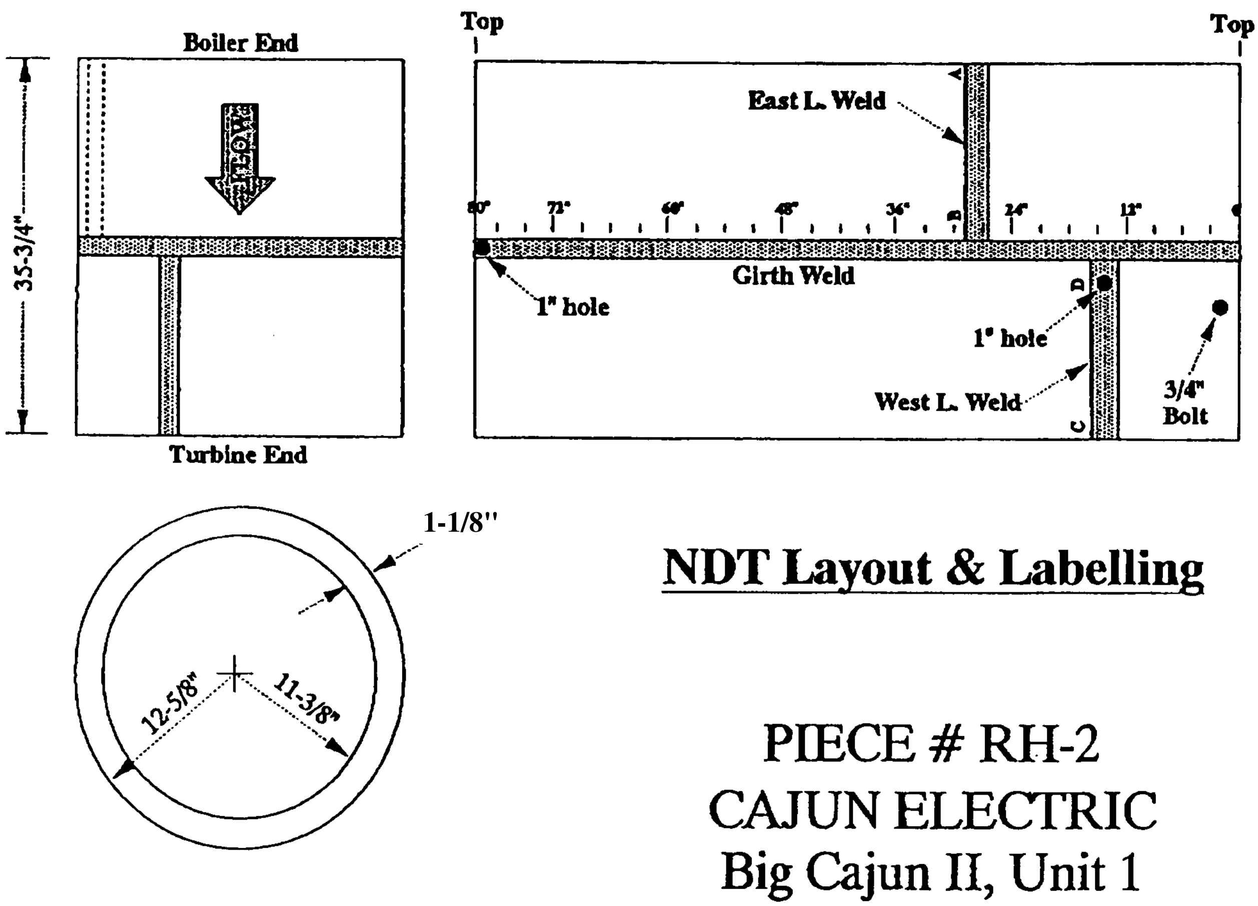

Figure 2 Layout of the Spool Piece for Nondestructive Testing.

The downstream end of the spool piece was polished and etched to reveal the weld profile of the longitudinal seam weld to facilitate the UT inspection (Figure 3). The double-vee geometry was seen and the cusp located approximately 3/8" from the I.D.

The internal surface of the pipe was covered with a layer of magnetite 7 to 10 mils thick. No visual evidence of unusual corrosion or erosion was found. A discontinuity in the joint preparation of the girth weld was also observed at the I.D. of the pipe. The end preparation shows a non-uniform counterbore on the upstream side of the weld (Figure 4). This observation is significant because an unanticipated geometric discontinuity could provide false indications during UT inspection, particularly since it would not be indicated on the original spool piece drawings.

Wet Fluorescent Magnetic Particle Inspection

Wet fluorescent magnetic particle inspection of the welds at I.D. of the pipe revealed no indications.

Radiographic Inspection

Radiographic gamma-ray (Ir 192) inspection of the two longitudinal weld seams was done using Type I film. The girth weld was shot panoramically. All three of the welds were found to be acceptable by code standards (See Ref. 2). The only features of note were iden-

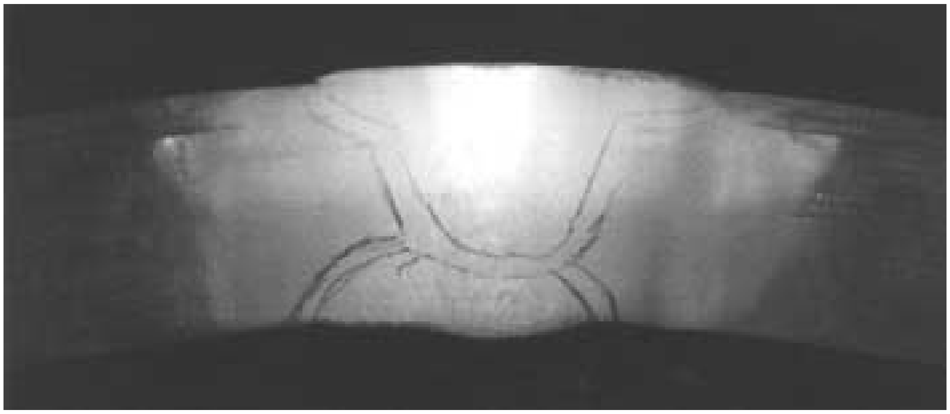

Figure 3 Macroetched, Cut End of the Downstream End of the Spool Piece, Showing the Asymmetry of the Double-V Seam Weld.

Figure 4 Internal Surface of the Spool Piece Showing Nonuniform Counterbore on the Upstream Side at the Girth Weld.

tified as porosity in the girth weld. These features were also detected by UT, and later identified by optical metallography as lack of root fusion.

Ultrasonic Testing

The ultrasonic inspection was done in accordance with EPRI guidelines. Initial zero degree longitudinal wave (straight beam) inspection was done at a distance about 6" from each side of the weld. This is performed to search for laminar reflectors in the weld and heat affected zone (HAZ), however, none were found. The shear wave (angle beam) analysis was done using a 2.25 MHz, 1/2" diameter transducer, fitted with 45° and 60° wedges. A 70° scan was not practical due to the curvature of the pipe. The shear wave examination was accomplished on both sides of the weld.

A recurring, linear indication was detected on one side of the upstream longitudinal weld (Figure 5a). The indication was found to be approximately 14" in length, starting at the top cut edge of the spool piece, with the signal trailing approximately 5" from the centerline of the girth weld. The indication was found with the 45° scan from the opposite side of the weld at a sound path of 3-1/2". The signal could not be displaced by repeated damping. Shallow, angled grinding of the weld toe at the top of the pipe resulted in the disappearance of the signal. Subsequent electropolishing and WFMT revealed no visual indications. A similar indication, only 1/4" in length, was found on the same side of the downstream longitudinal seam weld (Figure 5b). These indications were considered to be significant. A metallographic section was taken through the "upstream" indication for further analysis by optical microscopy.

The ultrasonic inspection of the girth weld showed one indication which was typical of porosity (Figure 6). This indication was found to be acceptable and would warrant no further action, as was also determined by RT. The non-uniform counterbore at the I.D. of the weld produced the appearance of a root signal, which could be clearly identified as an extraneous reflector because the surface distance (the distance from the exit point of the sound wave from the probe to the center of the weld) was too long to be in the weld zone. However,

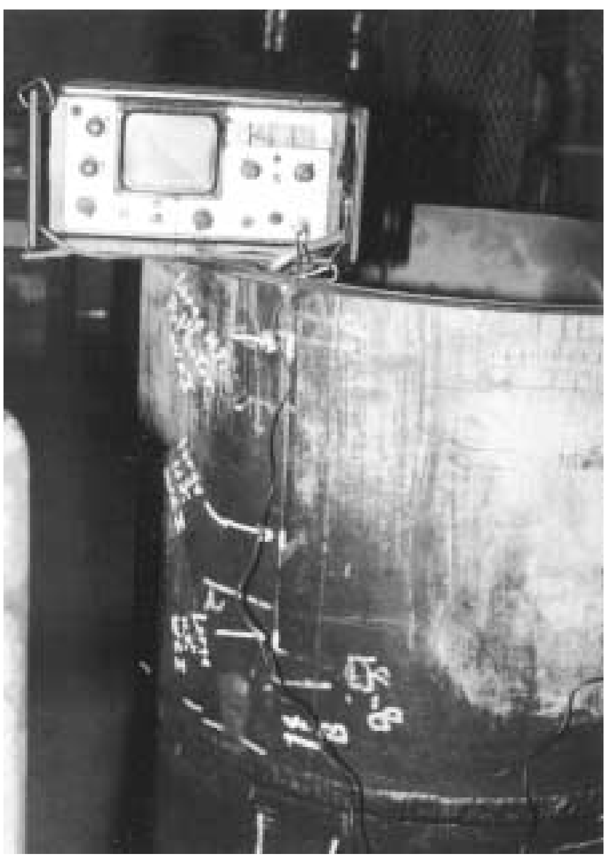

Figure 5a Upstream Leg of the Seam Weld Where a 14" Long Indication Was Seen on One Side of the Weld as Marked.

Figure 5b Overview of the Spool Piece Showing the 1/4" Long Indication on the Downstream Leg of the Long Seam.

field inspection of this weld would yield an unknown indication without access to the internal surface of the pipe or detailed piping drawings.

A sketch which summarizes the results of the UT and RT inspections is shown in Figure 6.

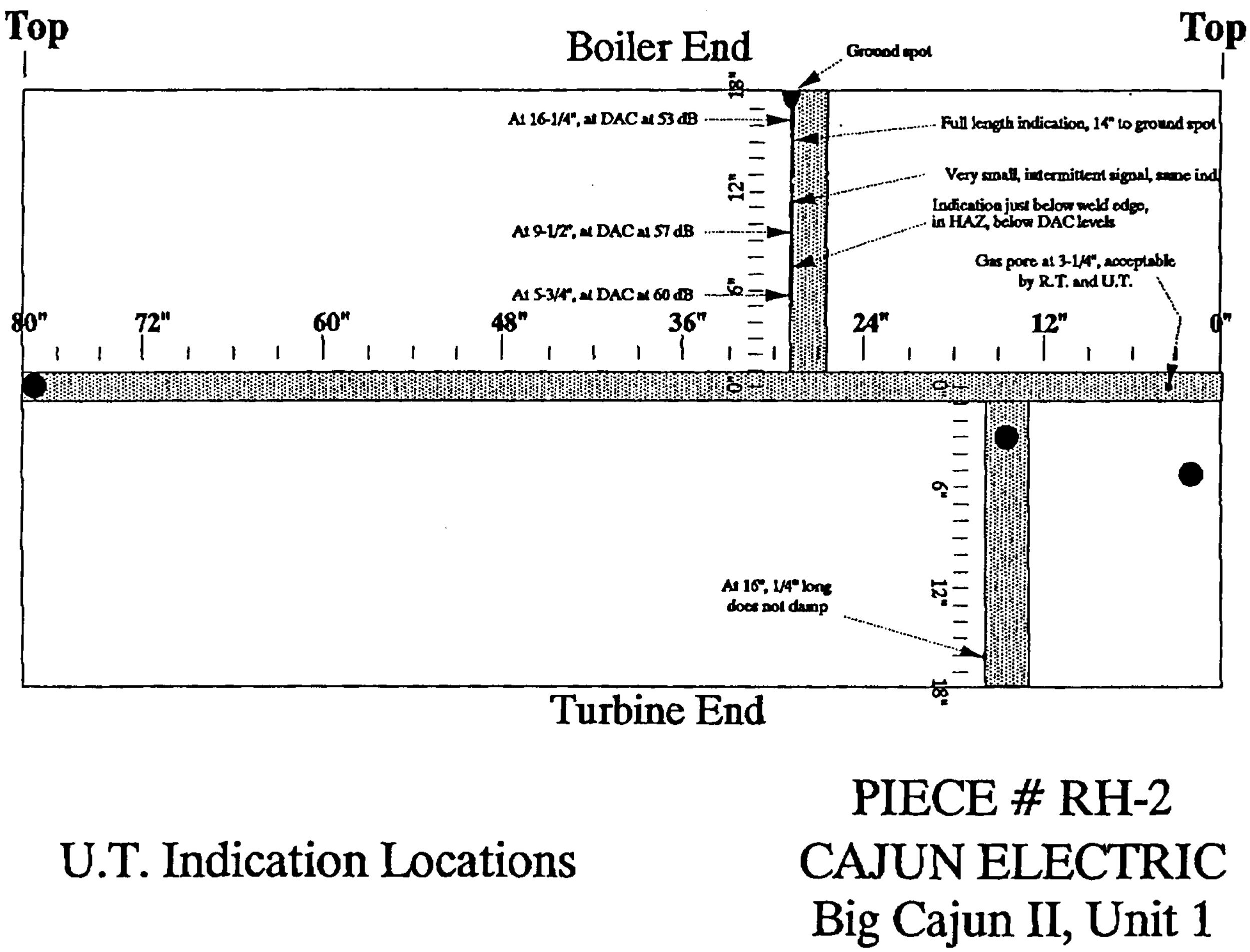

Figure 6 Sketch Showing the Locations of the UT and RT Indications on the Spool Piece.

TASK TWO: PHYSICAL AND CHEMICAL EVALUATION

Optical Metallography

Two full-cross-section metallographic specimens were removed from the spool piece, one from the longitudinal seam and the other from the girth weld. The locations of each were chosen based on the findings of the NDT. A transverse section was made through the upstream longitudinal weld seam at a location corresponding to a strong UT indication which had been detected just below the O.D. in the HAZ/fusion line region of the weld. A transverse section was also made through the indication suspected to be porosity as found by UT and RT techniques in the girth weld. Each specimen was metallographically prepared for optical microscopy.

Photomacrographs of the two metallographic samples are shown in Figure 7. No obvious HAZ is seen for the longitudinal seam weld which indicates that it has likely been subject

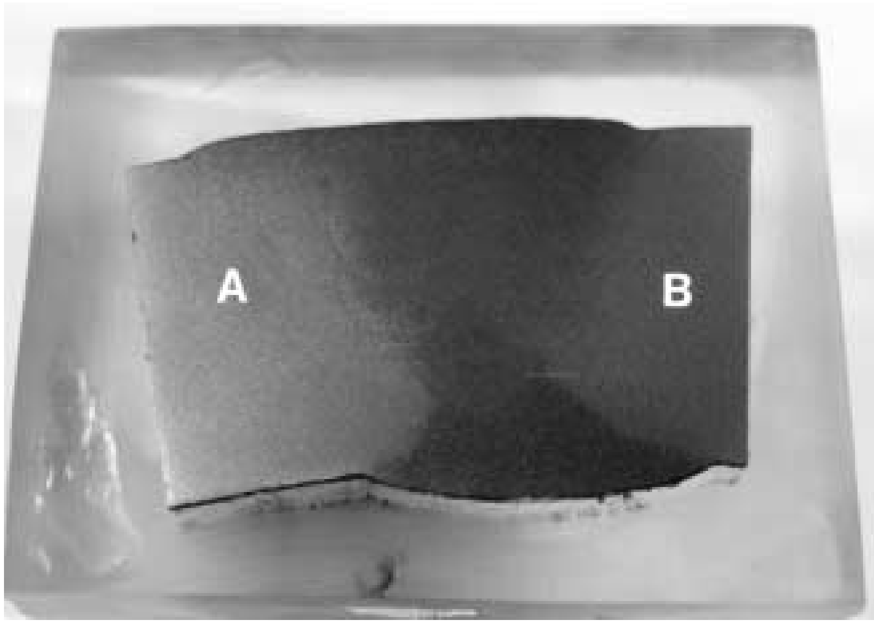

Figure 7a Photograph of Macroetched Metallographic Specimen of the Longitudinal Seam Weld

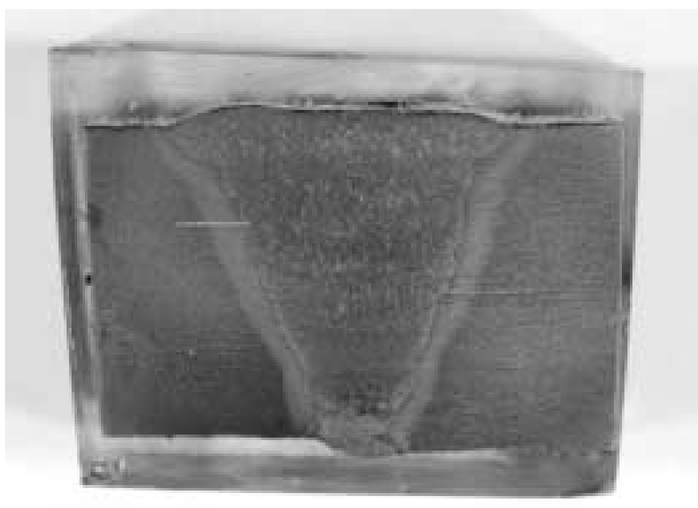

Figure 7b Photograph of Macroetched Metallographic Specimen of the Circumferential Weld.

to a post-weld normalizing heat treatment. In comparison, the HAZ is readily apparent for the circumferential weld which indicates that it has received a subcritical post-weld heat treatment.

The microstructure of the longitudinal seam weld shows no evidence of creep damage at magnifications up to 1000X. A high density of nonmetallic inclusions was found along the fusion line of the weld, including in the cusp region (Figures 8a and 8b). Mild intergranular oxidation is present at both I.D. and O.D. surfaces. No evidence of gross weld defects was seen. The base metal consists of some lamellar pearlite and a dispersion of fine spheroidized carbides in a ferritic matrix (Figure 8c). The presence of lamellar pearlite in the microstructure, typically seen in new material, indicates that the pipe base metal has not been significantly degraded by service temperatures.

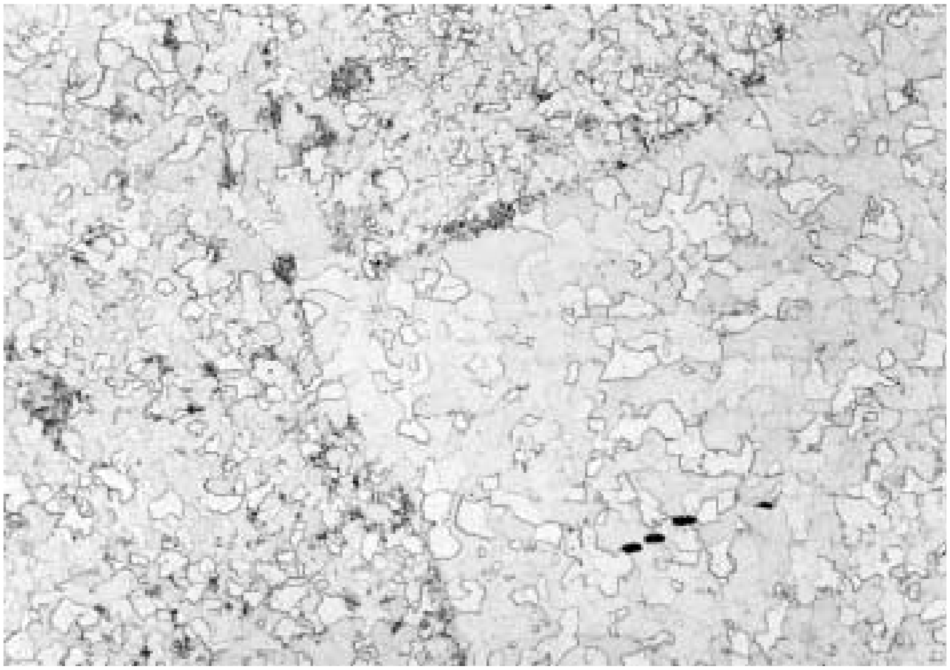

Figure 8a Microstructure at the Cusp of the Long Seam Weld (50X)

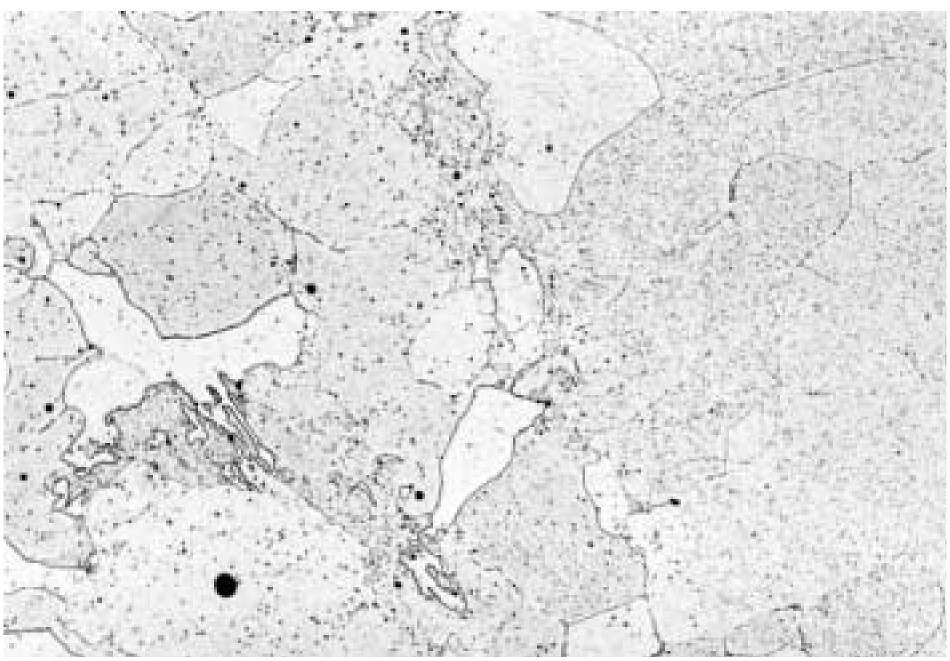

Figure 8b Detail of the Cusp Microstructure Showing a Higher Density of Nonmetallic Inclusions in the Weld Metal (left) Compared to the Base Metal (right) (400X)

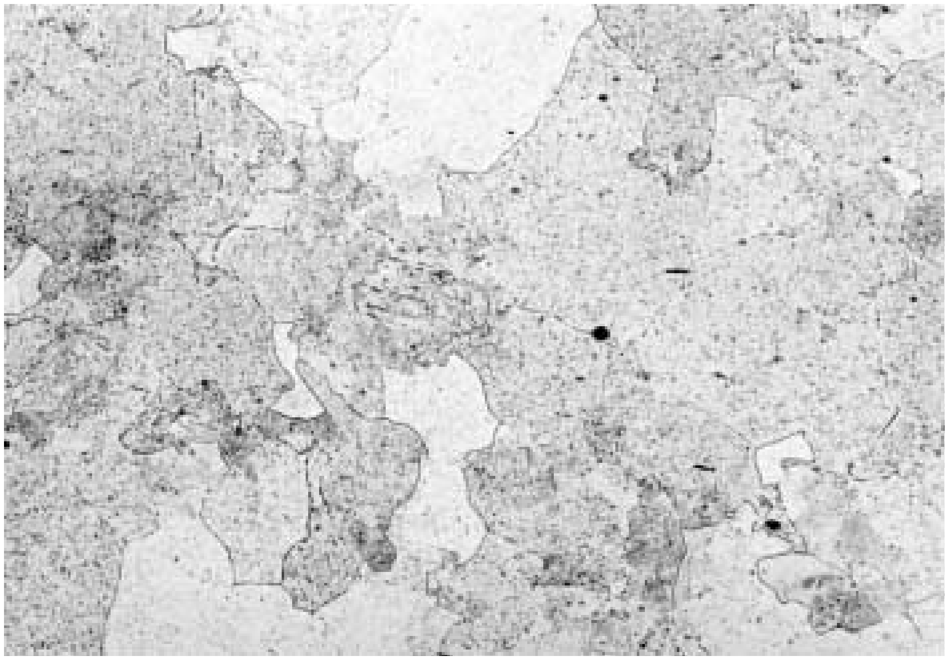

Figure 8c Detail of the Base Metal Microstructure Showing Some Lamellar Pearlite and Spheroidized Carbides in a Matrix of Ferrite. (400X)

The microstructure of the girth weld showed no evidence of creep damage (Figures 9a and 9b). The indication found by RT and UT suggested to be porosity was found to be lack of root fusion (Figure 9c). No evidence of creep damage was observed in association with this defect. The microstructure of the base metal is similar to that observed near the longitudinal seam weld (Figure 9d).

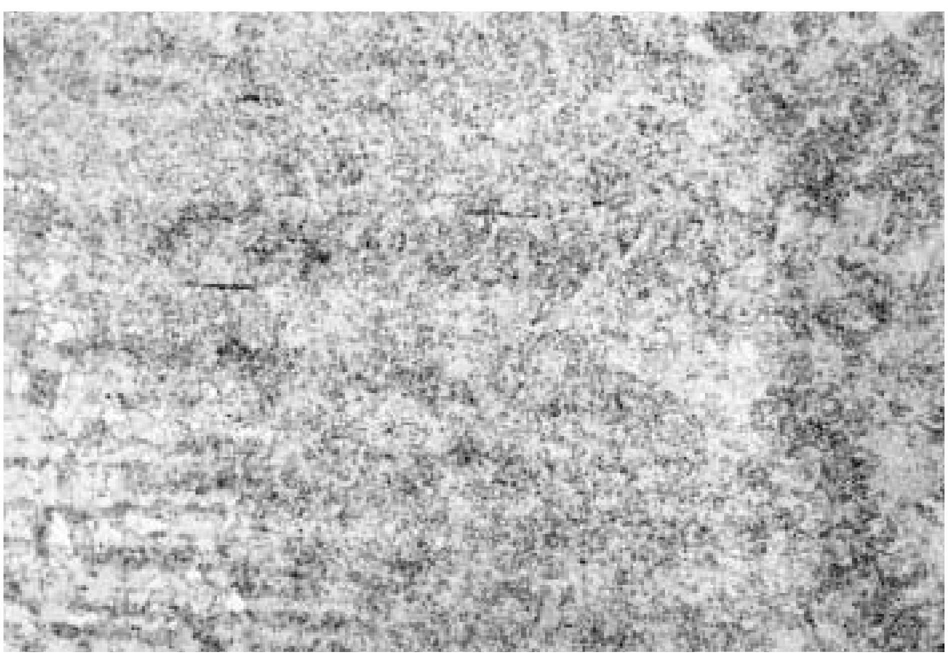

Figure 9a Overview of the Base Metal/HAZ/Weld Metal Interface of the Circumferential Weld. (50X)

Figure 9b Detail of the HAZ at the O.D. of the Sample Showing Intergranular Oxidation But No Evidence of Creep Damage. (400X)

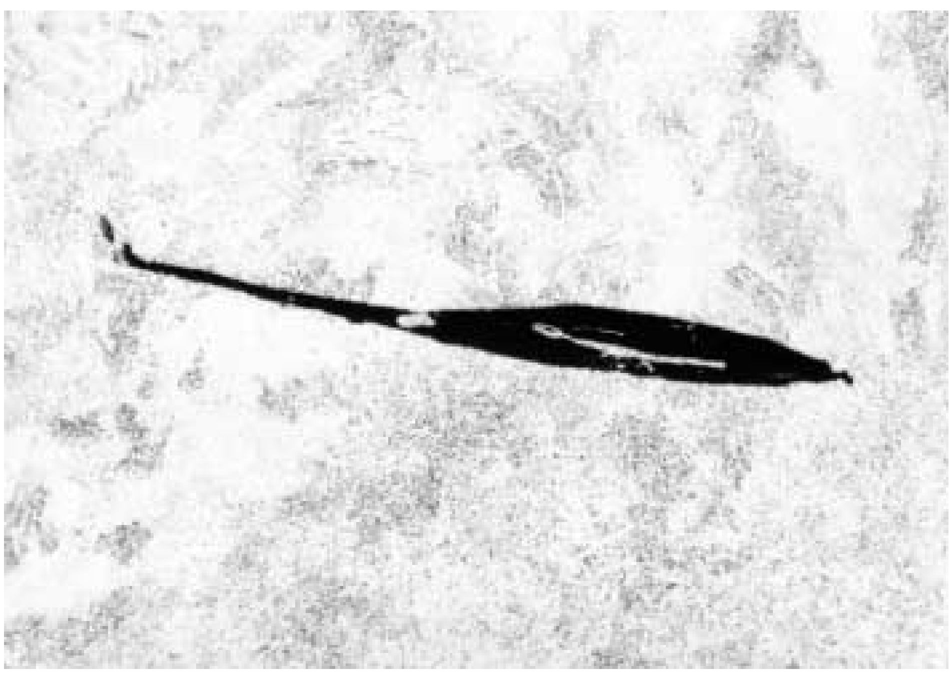

Figure 9c Overview of the Lack of Fusion Defect in the Circumferential Weld. (50X)

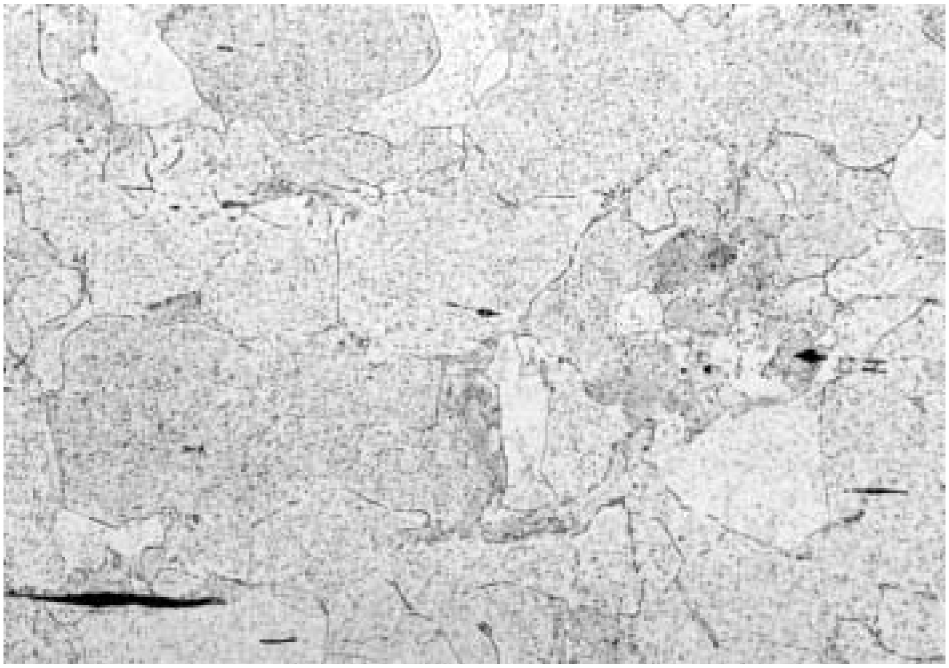

Figure 9d Detail of the Pipe Base Metal Showing Some Lamellar Pearlite and Spheroidized Alloy Carbides in a Matrix of Ferrite. Note Stringer Inclusions. (400X)

Spectrochemical Analysis

The results of the chemical analyses of the pipe base metal and the long seam weld metal are summarized in Table 1. The compositions of ASTM SA387-Grade D alloy steel pipe and ASME SFA-5.23, AWS FXPX-EB3-B3 electrode composition are given for comparison, respectively. The pipe base metal composition satisfies the ASTM requirements. The long seam weld metal sample also meets composition requirements, with the exception that the chromium content is slightly low. The actual weld filler metal used may have been within

Table 1 Chemical Analysis of Pipe and Long Seam Weld Metal Samples

Element	Pipe Base Metal, wt. %	ASTM A387-Grade D, wt. %	Longitudinal Weld Metal, wt. %	ASME SFA-523-AWS B3 wt. %
C	0.10	0.15 max.	0.067	0.12 max.
Mn	0.39	0.27 - 0.63	0.86	1.20 max.
P	0.009	0.035 max.	0.015	0.030 max.
S	0.016	0.040 max.	0.014	0.040 max.
Al	0.011	–	0.013	–
Si	0.21	0.50 max.	0.36	0.80 max.
Cr	1.92	1.88 - 2.62	1.94	2.00 - 2.25
Mo	0.96	0.85 -1.15	0.91	0.90 - 1.20
0_2	–	–	0.11	–

specification; however, certain fabrication techniques can result in the loss of reactive elements, such as chromium.

The oxygen content of the long seam weld metal is consistent with that resulting from the use of an acid flux. Welds made with an acid flux generally contain oxygen in the range of 0.07 to 0. 1 % (See Ref. 5). Acid flux usage during original fabrication has been theorized to increase the propensity for creep damage along the fusion line and at the weld cusp in some cases, when associated with a high inclusion density (See Ref. 3).

Scanning Electron Microscopy

The metallographically-prepared specimens of longitudinal seam weld and the stress-rupture tests were examined in the scanning electron microscope (SEM). Selected inclusions were characterized by energy dispersive X-ray analysis (EDS).

The weld metal inclusions of the longitudinal seam weld were found to be composed largely of manganese, silicon, aluminum, oxygen and sulfur (Figure 10).

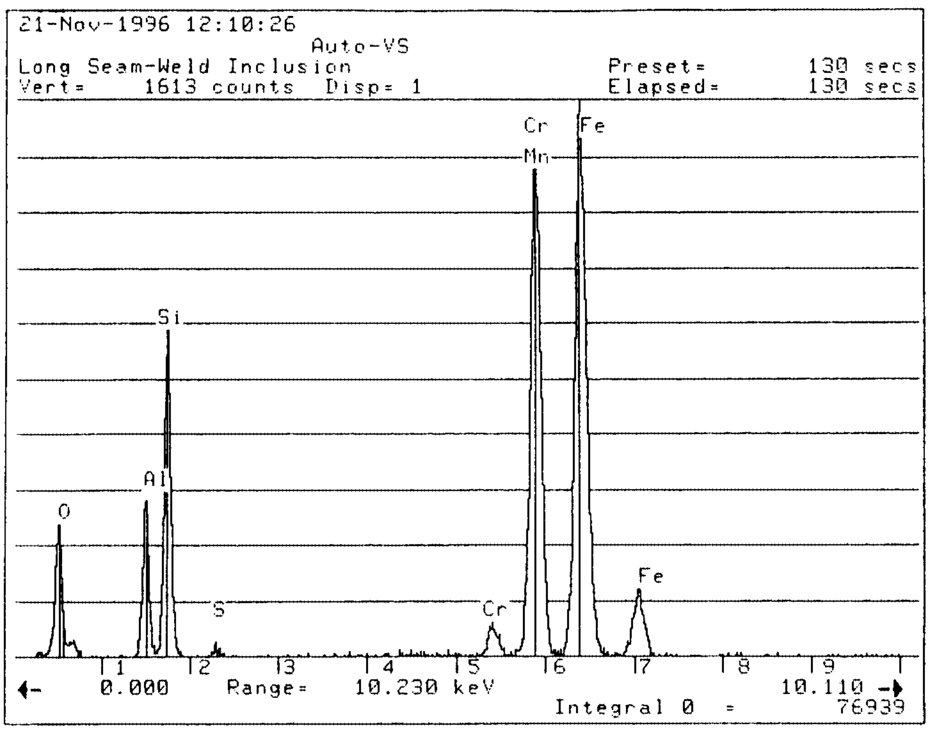

Figure 10 EDS Spectrum of Representative Long Seam Weld Metal Inclusion.

Examination of the stress-rupture specimens showed that cavity nucleation in the HAZ of the longitudinal seam weld was generally associated with an inclusion (Figure 11). EDS analyses of these inclusions showed that they are largely manganese and sulfur-rich (Figure 12).

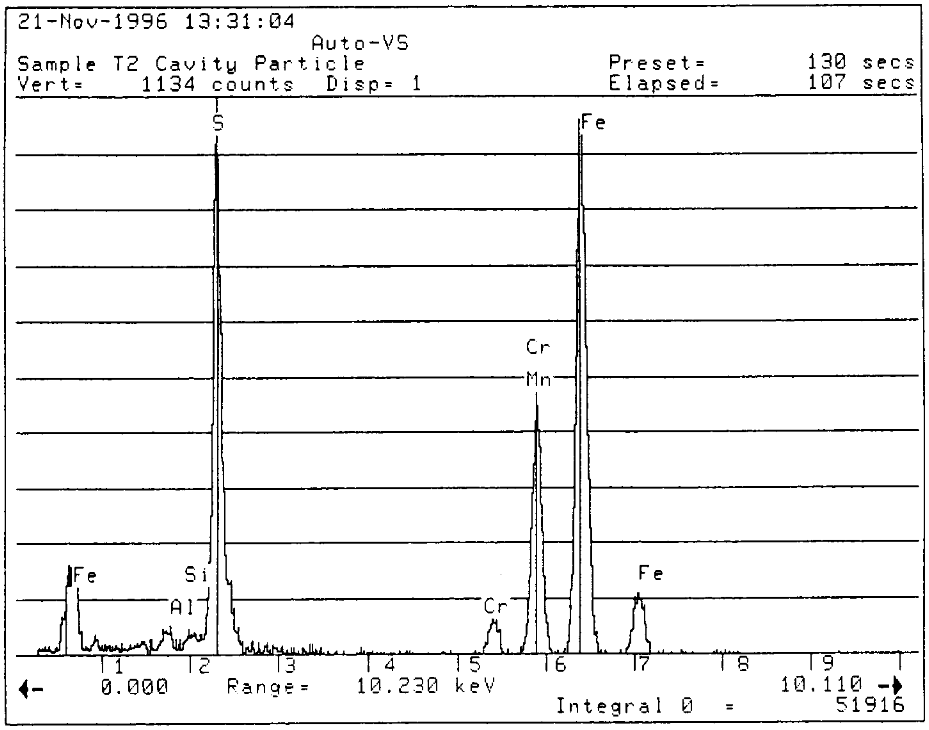

Figure 11 EDS spectrum of a Representative Particle Associated with a Cavity in the Stress-Rupture Sample, T2. Particle Seen in Figure 12.

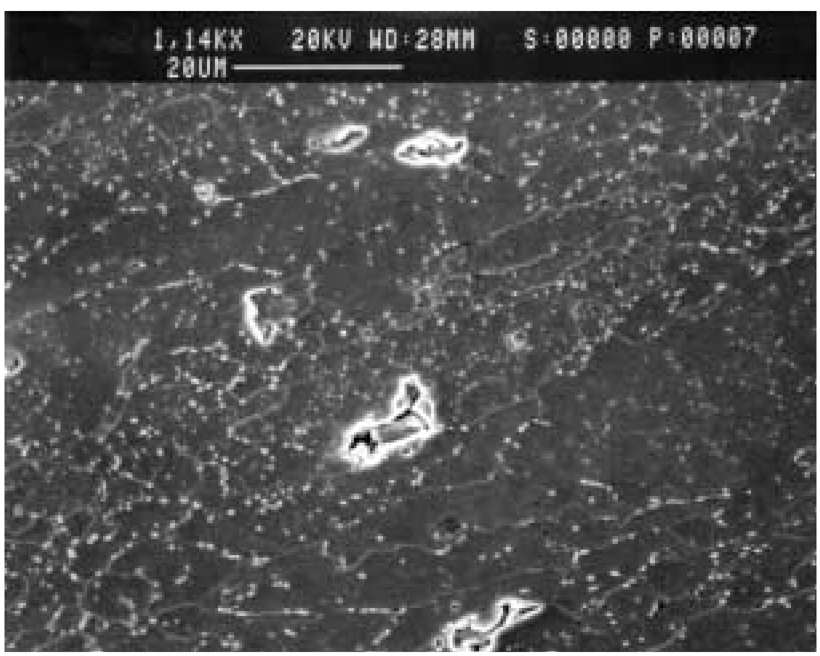

Figure 12a SEM Micrograph of Stress-Rupture Sample T2 Showing Cavity Nucleation at Nonmetallic Inclusions in the HAZ.

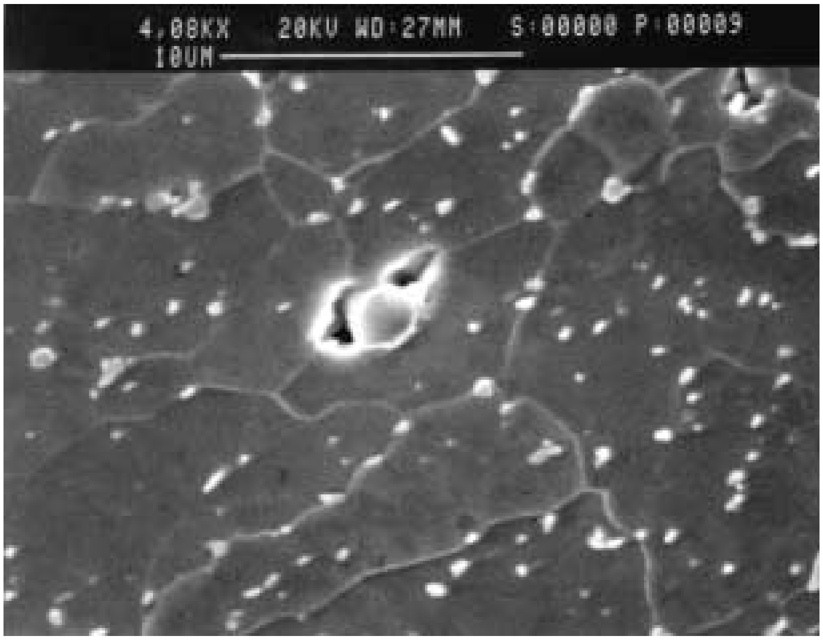

Figure 12b SEM Micrograph of Stress-Rupture Sample T2
Showing Cavity Nucleation at Nonmetallic Inclusions in the HAZ.

TASK THREE: MECHANICAL TESTING

The location of the mechanical test specimens are shown in Figure 13a, oriented perpendicular to the downstream leg of the longitudinal weld. Specimens T1 and T2 are the stress-rupture samples. Four of the six specimens designated C1 through C4 are used for testing elevated temperature toughness and creep-crack-growth. Figure 13b shows the macroetched blanks prior to preparation of the cross-weld specimens.

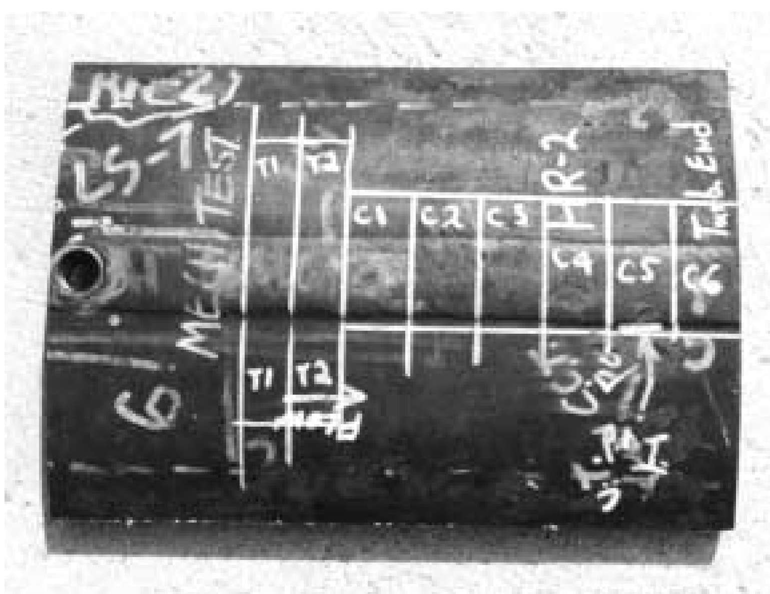

Figure 13a Orientation of the Stress-Rupture (T1 and T2), and Creep-Crack-Growth and J_{IC} Specimens (C1 through C6) on the Downstream Leg of the Long Seam.

Figure 13b The Macroetched Faces of the Specimens, Showing the Location of the Double-V weld.

Stress-Rupture Testing

Two blanks, oriented across the downstream leg of longitudinal weld, were machined into tensile specimens with a 1/4" diameter by 2" long gage section. The specimens, designated Tl and T2, were located so that the welds and heat-affected zones were in the gage section. The specimens were dead-weight loaded in tension in standard creep test frames and heated in air using a standard laboratory test furnace. The tests were accelerated by using 1225°F and 1250°F test temperatures, which are well above maximum service temperatures, and a stress of 7 ksi. A value of 7 ksi was chosen so that the results could be compared directly with those of a past study conducted for the Electric Power Research Institute (See Ref. 4), as may be seen in Figure 14.

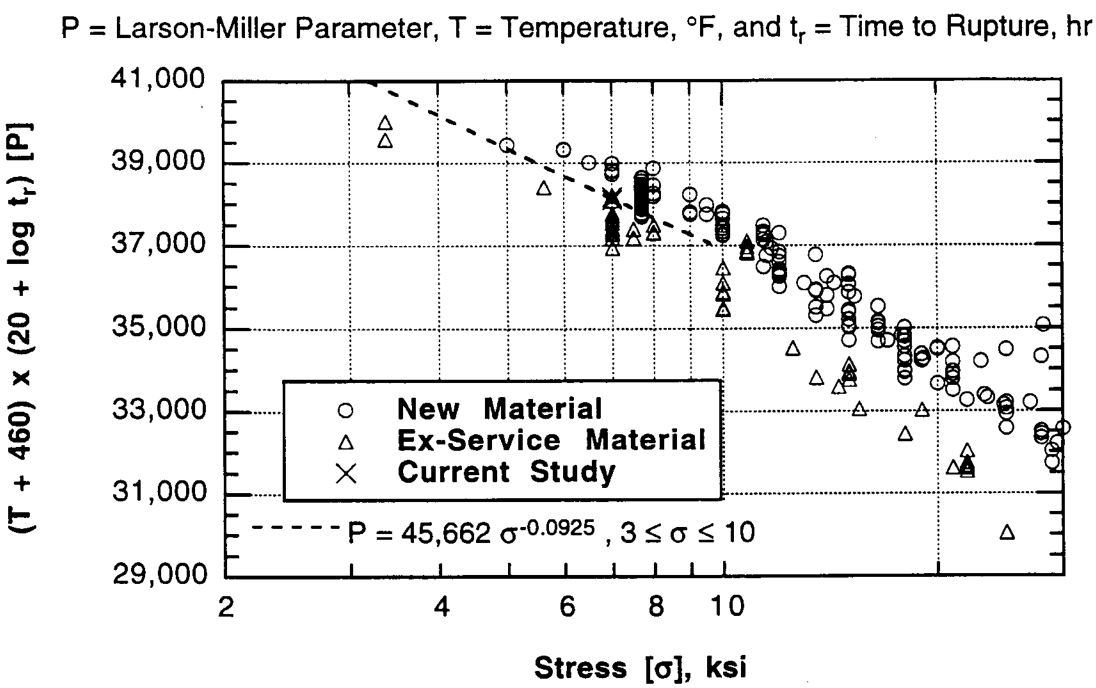

Figure 14 Results of the Stress-Rupture Tests Compared With Data From EPRI-TR-101835

Sample Tl failed after 213.9 hours at 1250°F and Sample T2 failed after 409.0 hours at 1225F. The calculated Larson-Miller parameters are given in Table 2. A substantial amount of ductility is seen in both samples. Optical metallography of the stress rupture test specimens showed that the fracture occurred through the HAZ (Figure 15). In addition, aligned cavities were observed in the weld metal at prior austenite grain boundaries.

From the results of the testing of Samples T1 and T2, the Larson-Miller parameters fell near the upper bound of results for ex-service material at 7 ksi in the past EPRI study. In addition, the results of the current study fall slightly below the mean values for new 2-1/4 Cr-1 Mo material as tested in the EPRI study.

Based on the mean diameter formula, the stress value of 7 ksi corresponds to an internal pressure of 652 psig. At 1015F, the average Larson-Miller parameter value of 38,140 yields an average stress-rupture life of 721,000 hours. Therefore, these results indicate that the stress-rupture life of the longitudinal seam weld (downstream leg) has not been seri-

Table 2 Results of Stress-Rupture Tests at 7 KSI

Specimen	Test Temp, °F	Time to Rupture, Hrs.	Elongation, Pct.	Reduction of Area, Pct.	Larson-Miller Parameter*, C=20
T1	1250	213.9	17.8	69.3	38,185
T2	1225	409.0	15.7	70.8	38,101 Ave.=38,143

* Larson-Miller Parameter = (T + 460) (log tr + C); T is temperature in degrees F and tr is time to rupture in hours.

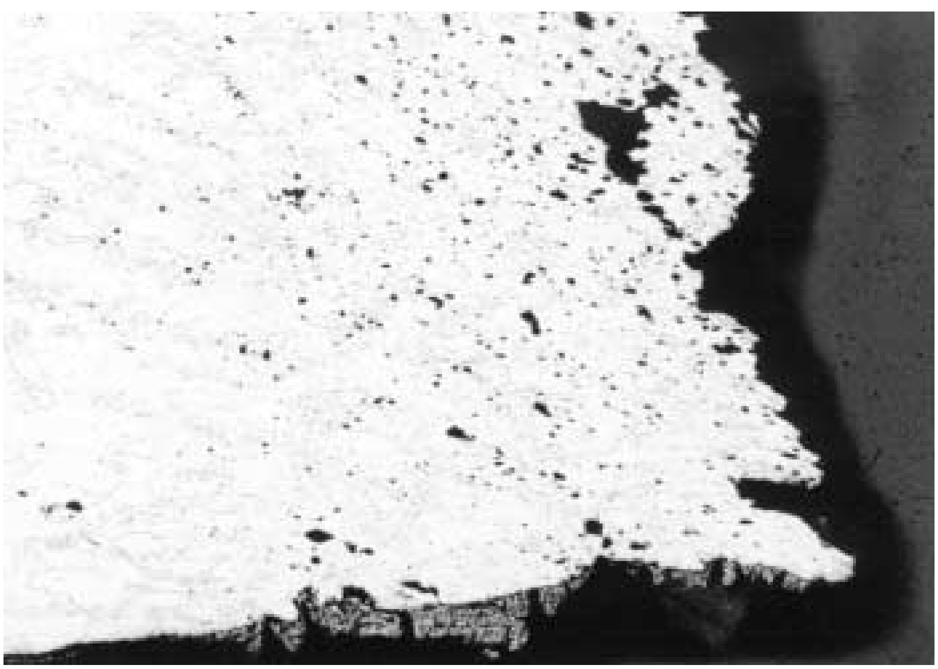

Figure 15a Micrographs of the Stress-Rupture Specimen, T1, Showing That Failure Occurred Through the HAZ of the Long Seam Weld. (50X)

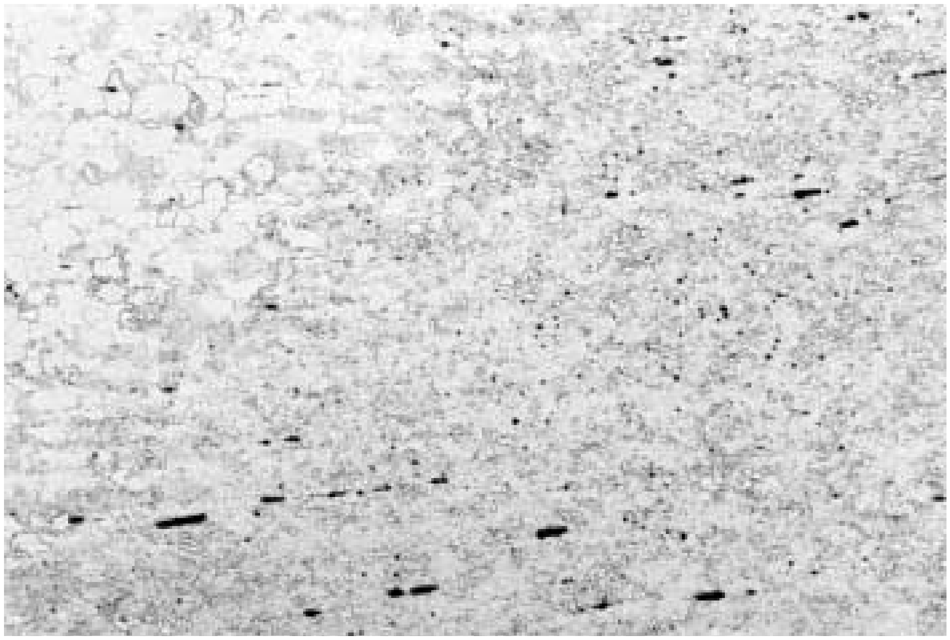

Figure 15a Micrographs of the Stress-Rupture Specimen, T1, Showing That Failure Occurred Through the HAZ of the Long Seam Weld. (50X)

ously degraded by past service exposure. The results suggest that the material should have adequate remaining life under steady-state conditions; that is, without overheating, overloading, excessive cycling or material defects.

Elevated Temperature (J) Fracture Toughness Testing

J fracture toughness tests were performed on Specimens C3 and C6. The purpose of this test is to determine the elevated temperature toughness of the material under elastic-plastic fracture conditions. The toughness is used to estimate the critical through-wall flaw size which will initiate unstable fracture of the pipe. This information could be used in the detection stage to assess the immediate danger of any cracks.

Two 1/2T compact-tension (CT) specimens had been machined from the specimens. The notches of these CT specimens were located near the fusion line of the seam weld and fatigue pre-cracked to produce a sharp starting notch. Specimens C3 and C6 were heated to temperatures of 1005°F and 1015°F in air, respectively, before testing. The testing and data analysis were done in accordance with procedures specified in ASTM E813 and E1152.

In accordance with ASTM E813, provisional values of J fracture toughness (J_Q) are obtained. The J_Q values for Specimens C3 and C6 are 123 (712) and 94 (544) kJ/M^2 (lb./in.), respectively. In order for J_Q to be a valid J_{IC} fracture toughness, specimen thickness, remaining ligament and near-surface crack length requirements of ASTM E813 must be satisfied. For the current study, these criteria were not met and therefore the J_Q are not valid J_{IC} values. However, the measured J_Q values are used as engineering approximations of fracture toughness, albeit conservative.

The results compare well with other J_Q values for 2-1/4 Cr - 1 Mo steel at temperatures near 1000°F as reported in the literature (See Ref. 4). As may be seen in Figure 16, the J_Q value for specimen C6 is lower than that for Specimen C3, which is attributed to a variation in microstructure and not to the slight difference in test temperatures. The crack path of the Specimen C6 appears to follow the fusion line of the long seam weld, and that of Specimen C3 does not.

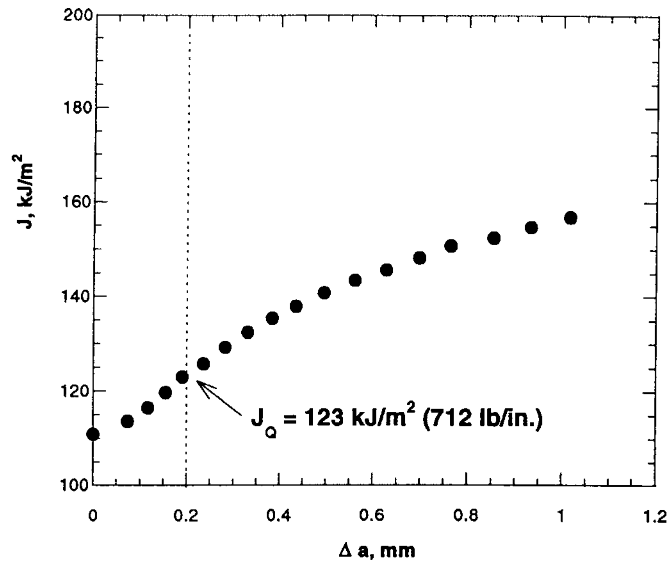

J-R Curve for Specimen C3.

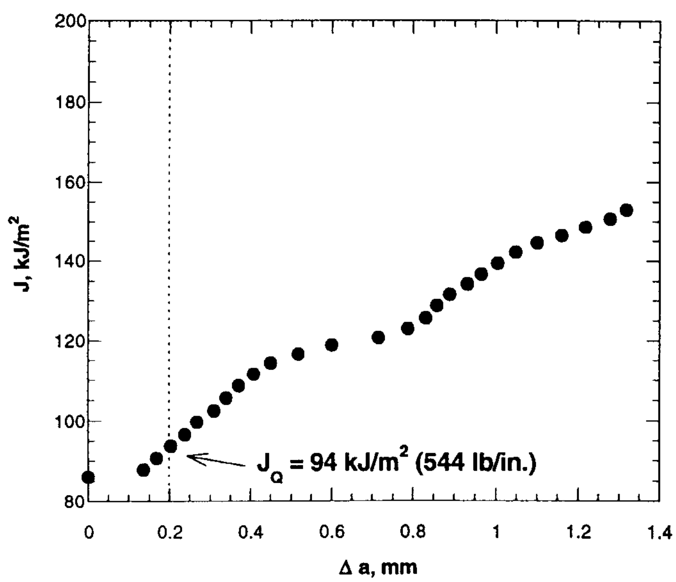

J-R Curve for Specimen C6.

Figure 16 The J-R curves (plots of J versus da) were developed from the measured data and used to determine J_Q fracture toughness at da=0.2 mm.

Creep-Crack-Growth (C*) Testing

Creep-crack-growth (C*) testing was carried out in order to determine the rate at which a creep crack would propagate under elastic-plastic conditions.

Two 1/2T compact-type (CT) specimens were machined from the long seam weld blanks, C2 and C4.The notch of each specimen was located near the weld fusion line and fatigue pre-cracking provided a sharp starting notch. Before the specimens were tested, each was held at a temperature of 1015°F for 30 minutes. The specimens were loaded to 1200 lbs. at temperature. Load-line displacement and DC potential drop (used to obtain crack extension data) were measured. The measured data was used to develop creep-crack-growth information in accordance with ASTM E1457-95.

The creep-crack-growth data for Specimens C2 and C4 are presented in Figure 17. High crack growth rates (da/dt) were obtained for Specimen C2 under these test conditions, which failed in only one hour. In contrast, much lower crack growth rates were measured for Specimen C4, which failed in 527 hours. The accelerated fracture of Specimen C2 compared with that of Specimen C4 is most likely a result of differences in material microstructure, since there were no significant differences in the original conditions of the test specimens. The creepcrack-growth data for both specimens falls within the lower and upper bound for data for 2-1/4-1 Mo base metal tested under similar conditions. Since the crack path for the test specimens was through the weld metal, the results indicate that creep-crack-growth resistance of the weldment specimens has not been significantly affected by service exposure.

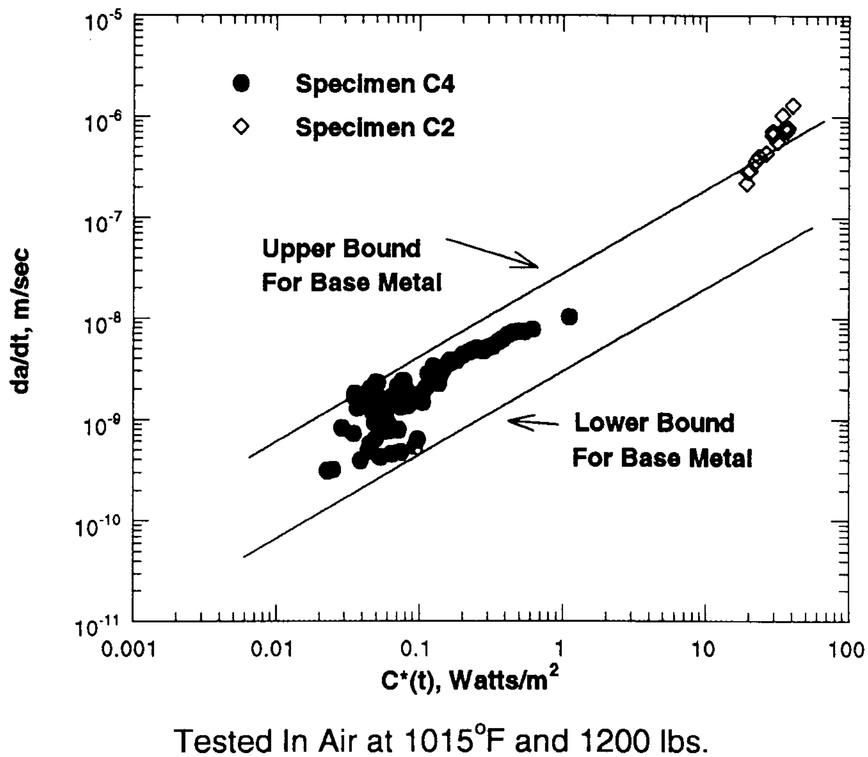

Figure 17 Creep-crack-growth data for Specimens C2 and C4

Remaining Creep Life Assessment

Using the data developed in this study, and reported typical operating temperature and pressure data, simplified assessments of the remaining creep life of the hot reheat piping material was performed. One assessment is based on the creep-rupture testing and uses the linear life fraction rule; the other is based on creep-crack-growth.

The testing of the weldment specimens taken from the spool piece revealed the following:

(1) minimum creep rupture strength is represented by the lower bound creep rupture strength for new 2-1/4 Cr - I Mo steel (Figure 14).

(2) secondary creep rate was represented by the typical behavior of service exposed 2-1/4 Cr - I Mo steel, and

(3) maximum creep-crack-growth rate was represented by the upper bound creep-crack-growth of 2-1/4 Cr - I Mo base metal (Figure 13b).

These findings show that the weldment specimens tested fall well within the reported industry findings as catalogued by EPRI for the stress-rupture and creep-crack-growth behavior of 2-1/4 Cr - 1 Mo steel. Even more optimistically, it shows that the test results of the weld metal specimens are comparable to those for base metal. In order to predict remaining life of the steam line, an I.D. of 23 inches and a minimum wall thickness of 1.124 inches were used in the calculations. Operating records supplied by Cajun Electric for the time period of August 14 through 17, 1996, were used obtain pressures and temperatures for computation of the minimum remaining creep-rupture life of the steam line. The potential for fracture initiation was assessed by the using only the pressure-induced hoop stress, and system-induced stresses were assumed to be negligible.

Using the linear life-fraction rule, a creep damage fraction of 2.52 x 10^5 was calculated for the 4-day period of typical operation. This, in turn, was extrapolated to a total remaining creep rupture life of 3,811,000 hours. This very long remaining creep rupture life explains why the creep-rupture tests showed little evidence of creep damage.

The creep-crack-growth model was based on an average operating temperature of 1000°F, which was calculated from the 4-day period of operating conditions. At this temperature, an average pressure of 509 psig was calculated to give a creep rupture life of 3,811,000 hours. Cajun reported that for 1994, 1995 and 1996, there was an average of 7620 hours of past operation per year. For 1997, Cajun had predicted that there would be 7230 hours of operation. Since more frequent cycling would be expected to produce shorter predicted life, remaining creep lives were computed for 2, 4, 6 and 12 equal cold start-stop cycles per year. The crack length-to-depth ratio (L/d) was assumed to remain constant for initial growth. An initial crack depth of 0.1 inches was chosen. The crack is assumed to be longitudinally oriented and located at the I.D. of the pipe in the vicinity of the weld. The final crack depth was determined to the lesser of the two values of either the minimum ordered wall thickness (1.124-inches) or the critical crack depth for a critical toughness (J) value of 500 lb./in. This value is the depth that would be necessary to initiate fracture for steady operation at 1001°F and 509 psig. This value is 1.124" for L/d = 10, and is 0.684-inches for L/d = 50.

The results of the calculations are given in Table 3, which summarizes the life values for components which contain an initial crack depth of 0.1 inches. In all cases, the remaining lives are greater than 100,000 hours (13.1 years) when there are no more than 2 cold stop-start cycles per year. For the worst case, an L/d ratio of 50/1 and 12 cycles per year, the remaining creep life is still more than 64,000 hours (8.3 years). Even longer lives would be expected for crack L/d ratios of less than 10, and, as stated earlier, for less frequent cycling.

The predicted remaining lives indicate that the average operating pressure of 509 psig and temperature of 1001°F for this steam piping are reasonable based on the properties of the specimens evaluated in this study, and the conditions assumed in the analyses. On this basis, normal maintenance, inspection and evaluation of the piping is recommended.

Table 3 Calculated Remaining Creep-Crack-Growth Lives

Type of Operations	Number of Cycles Per Year	Length of Cycle, Hours	Total Remaining Life for L/d Ratio[a], Hours		
			L/d=2[b]	L/d=10[b]	L/d=50[c]
Past	2	3810	761,000	311,000	115,000
	4	1905	709,000	255,000	97,100
	6	1270	601,000	218,000	85,100
	12	635	429,000	159,000	64,400
Future	2	3615	721,000	307,000	114,000
	4	1808	695,000	250,000	95,600
	6	1205	587,000	213,000	83,500
	12	603	418,000	155,000	83,000

(a) L/d=crack length/depth and the initial crack depth is 0.1 inches
(b) Critical crack depth=1.124 inches
(c) Critical crack depth-0.684 inches

DISCUSSION AND CONCLUSIONS

The present study has followed current industry guidelines for detecting damage in the weldments of high energy piping. Based on the findings of the analyses and testing of the spool piece, the following conclusions are made for this component:

- Visual inspection yielded no evidence of gross defects in the spool piece. Unlike the inherent limitations of *in-situ* inspection of piping, laboratory analysis offered the obvious advantage of being able to examine the internal surface of the spool piece, by visual, nondestructive and destructive techniques. The most significant finding was the presence of a nonuniform counterbore at the I.D. of the girth weld (it does not go completely around the circumference of the pipe). This discontinuity was introduced during joint preparation of the pipe ends prior to welding. The counterbore is located 3/4-inch from the root face of the girth weld, at a location under the crown of the weld. This discontinuity provided a linear indication during the on-site inspection that was identified as a root center crack. In the field, this reflector would appear to be a root signal; however, the surface distance (the distance from the exit point of the sound from the probe to the center of the weld) was too long for this reflector to be in the weld zone. This indication was identified as a crack, both by ultrasonic testing (UT) and radiography (RT), since the internal surface of the pipe could not be seen in the field.

- Wet fluorescent magnetic particle inspection of the internal surface of the welds showed no indications. External WFMT (done in the field) revealed no indications.

- Indications were detected in the girth weld by both UT and RT. In the laboratory, the largest indication was identified as a fabrication-induced flaw, namely lack of root fusion, by metallographic examination. No evidence of creep damage was found to be associated with the flaw, when examined by optical microscopy.

- A recurring, linear (longitudinal) indication was detected by UT (in the lab) near the fusion line of the longitudinal seam weld, which has not been positively identified at this time. No evidence of either fabrication- or service-induced flaws was found by radiographic inspection, optical metallography or scanning electron microscopy. One potential cause of the UT indication is changes in grain size between the weld and the base metal HAZ, which can cause a reflector similar to an indication. Also, minute solidification cracks under the cap pass of submerged arc welds, known colloquially as "hat" cracks, could have escaped detection by metallography. This indication was not identified in the field, probably because EPRI guidelines for UT inspection of long seam piping had not been implemented at that time. EPRI guidelines (See Ref. 1) require that once a reference level is established, the scanning sensitivity is determined by increasing the gain by 14 dB.

- No evidence of creep damage was observed in the metallographically prepared specimens of the long seam or girth welds. The piping base metal showed only beginning-stage spheroidization indicating that the metal has not been significantly degraded by service temperatures.

- A significant concentration of nonmetallic inclusions was observed in the weld metal of the upstream longitudinal weld, particularly evident along the fusion line in the cusp region of the weld. Chemical analysis of the weld material showed that the oxygen content is consistent with the use of an acid type flux during original fabrication. Scanning Electron Microscope/Energy Dispersive X-Ray (SEM/EDS) analysis of weld metal inclusions in the longitudinal seam metallographic specimen showed that the spherical particles were largely composed of manganese, silicon, aluminum, oxygen and sulfur. Inclusions were found to be manganese and sulfur-rich. These inclusions are typical of those found in welds made by the submerged-arc welding (SAW) process. One study (Ref. 3) suggests that high concentrations of nonmetallic inclusions near the fusion line of long seam welds, as introduced by the SAW process and acid-type fluxes, may increase the likelihood for creep damage to initiate.

- Contrary to the observation of a high concentration of weld metal inclusions, the results of the cross-weld stress-rupture tests indicate that the stress-rupture life of the longitudinal seam weld has not been seriously degraded by their presence or by service conditions.

- Remaining creep life assessment was done using the results of the stress-rupture, high temperature (J) toughness, and creepcrack-growth testing carried out on specimen of the long seam weldment. The findings indicate that service temperatures and pressures have not significantly reduced the creep properties of the piping weldment , and furthermore, that the test results of the weldments are comparable to industry findings for 2-1/4 Cr -1 Mo base metal. Specifically, (1) the minimum creep rupture strength is represented by the lower bound of creep rupture strength for new 2-1/4 Cr -1 Mo steel, (2) the secondary creep rate (pre-cavitation stage) is represented by the typical behavior of service exposed 2-1/4 Cr - 1 Mo steel, and (3) the maximum creep-crack-growth rate was represented by the upper bound of 2-1/4 Cr - 1 Mo base metal.

- Remaining creep life was estimated using: (1) a simplified model based on the stress-rupture test results, and (2) a more conservative model in which a flaw has been introduced to the weldment via a machined notch and fatigue pre-cracking. In the first approach, a total remaining life of 3,811,000 hours was calculated using the linear life-fraction rule. In the second, the predicted remaining creep lives, using the creep-crack-growth model and typical operating parameters, were more conservative (e.g. for 2 cycles per year, 3615 hours each cycle, and a crack length-to-depth ratio of

2 [critical crack depth of 1.124"], a total remaining life of 721,000 hours is predicted, see Table 3).

- The creep-crack-growth model shows that the average operating pressure of 509 psig and temperature of 1001F for this steam piping are reasonable based on the parameters of the specimens tested and operational data reported. Adequate remaining life is expected under steady-state conditions and in the absence of material flaws or sustained, undue operational loading. Normal maintenance, inspection and evaluation of the piping is recommended at this time.
- A calibration block has been fabricated from the spool piece for future UT inspection of the Cajun piping.

REFERENCES

1. J. R. Foulds, R. Viswanathan, J. L. Landrum, S. M. Walker, “Guidelines for the Evaluation of Seam-Welded High Energy Piping”, EPRI TR-104631, January 1995.
2. ANSI/ASME B3 1. 1, Power Piping Code.
3. J.F. Henry, F.V. Ellis, C. D. Lundin, “The Effect of Inclusions as Controlled by Flux Composition on the Elevated Temperature Properties of Submerged-Arc Weldments,” Weld Tech 88 - Int. Conf. On Weld Failures, London, November.
4. C. W. Marschall, C. E. Jaske, B. S. Majumdar, “Assessment of Seam-Welded Piping in Fossil Power Plants,” Final Report EPRI TR-101835, Electric Power Research Institute, Palo Alto, California, December, 1992.
5. C. H. Wells, R. Viswanathan, “Life Assessment of High Energy Piping,” ASME Pressure Vessel and Piping - Decade of Progress, ASME, New York, NY, 1993.